Appl. Phys. B 58, 459–466 (1994)

Applied Physics B Lasers and Optics

Temperature Measurement using Degenerate Four-Wave Mixing with Non-Saturating Laser Powers

A.P. Smith, A.G. Astill

AEA Technology, Combustion Centre, 551 Harwell, Didcot, Oxfordshire OX11 0RA, UK
(Fax: +44-235/432404)

Received 19 November 1993/Accepted 22 February 1994

Abstract. We report the use of Degenerate Four-Wave Mixing (DFWM) in the OH $A^2\Sigma^+ \leftarrow X^2\Pi$ ($v' = 0 \leftarrow v'' = 0$) band for temperature determination in a propane/air flame using laser powers below the saturation level. We show that at these low power levels the dependence of the signal on the dipole moment for the transition has to be established before meaningful temperature data can be obtained. This presents a paradox in that the temperature has to be known before the form of the dependence on the dipole moment can be determined. Solutions to this paradox are presented. We also show that absorption of the laser beams in this OH band system cannot be neglected and that failure to correctly account for the absorption leads to a large over estimate of the flame temperature. Furthermore, we show that the accuracy of the absorption-corrected temperature is critically dependent on the accuracy with which the measurement position within the flame is known. Finally, the temperature calculated from DFWM spectra using the correct dipole moment power and absorption is compared to the temperatures obtained using Laser-Induced Fluorescence (LIF) and Coherent Anti-Stokes Raman Spectroscopy (CARS).

PACS: 82.40.Py, 07.20.Dt, 07.65.-b, 33.20.Lg

An understanding of any combustion process generally requires a knowledge of the fuel field, the oxidant field and the temperature field within the combustor. Laser-based optical diagnostics have been developed over a number of years with a view to acquiring this information [1]. The key features of these techniques are that they are noninvasive and can offer high spatial and temporal resolution. The two most widely used techniques are Coherent Anti-Stokes Raman Spectroscopy (CARS) and Laser-Induced Fluorescence (LIF). CARS has been developed over the last 15 years to the point that it is now virtually unrivalled as a single-point temperature diagnostic [2].

However, CARS is not able to record two dimensional images of the temperature distribution within a flame. LIF, on the other hand, is a proven imaging technique particularly for species mapping, and a variety of species including OH [3,4], NO [5], O_2 [6], CH and C_2 [7] have been imaged. More recently LIF has been extended to fill the thermometry gap left by CARS; namely that of temperature imaging. This generally involves imaging the OH distribution using two different excitation wavelengths and taking the ratio of the two images [8]. LIF however, is an incoherent technique which means that large area optical access is required and the detector must be close to the interaction zone.

In an attempt to overcome the limitations of both CARS and LIF, Degenerate Four-Wave Mixing (DFWM) is now receiving a great deal of attention as a complementary tool for combustion diagnostics [9]. DFWM is a nonlinear technique which has features in common with both CARS and LIF. Like CARS it uses three input waves to generate a fourth, coherent, signal wave. Like LIF, it utilises an electronic resonance which affords the technique a high sensitivity and it can be extended to two dimensions for imaging applications [10]. It is the combination of high sensitivity and coherence, coupled with the wide range of species that DFWM can detect, that give it possible advantages over the more established techniques. Examples of combustion species studied using DFWM include OH [11, 12], NH [13], NO [14], NO_2 [15] CH [16] and HCO [17].

In this paper we report an investigation of temperature measurement using DFWM spectroscopy of OH in atmospheric pressure flames at low laser powers. Previous work using NO has shown that the intensities of individual ro-vibrational lines show a dependence on the transition dipole moment of μ^x [18]. The value of x is itself found to be a function of laser intensity I. Similar studies on the OH molecule have, to date, shown that the dependence on transition dipole moment is μ^4 [13, 19]. This is in agreement with the usual assumption that the line intensities are proportional to the square of the one photon line strength. We show that this is not the case

(as in NO [18]) when $I \ll I_{sat}$ and that failure to take into account the power regime under which the data was taken can lead to significant errors in the measured DFWM temperature. This becomes important in imaging applications where expansion of the input beams to give a larger sample volume leads to lower values of I. Temperature measurements were made using CARS, LIF and DFWM in the same, reproducible flame which illustrate the potential problems of DFWM thermometry. We also show that absorption of both the input and signal beams in the flame has a larger effect on the measured temperature when using DFWM than when using LIF.

1 Experimental

Figure 1 shows a schematic of the experiment. We used a phase conjugate geometry with the backward pump formed by retro-reflection of the forward pump. A 20% beam splitter formed the probe beam which crossed the forward pump at an angle of $\approx 5°$ in the horizontal plane. The usual geometry was modified slightly by tilting the path of the backward pump beam down by a small angle ($\approx 0.1°$) in the vertical plane. This causes the path of the signal to be lowered by an equivalent amount below the probe beam because of the phase matching requirements of DFWM. Instead of using a beam splitter in the probe a prism can then be used to pick off the signal. This has the double advantage that all of the probe beam reaches the interaction zone and all of the signal reaches the detector. Furthermore, noise levels are significantly reduced by removal of the beam splitter.

A pulsed XeCl excimer laser (Lambda Physik EMG 101E) was used to pump a frequency-doubled dye laser (Lambda Physik FL3001) giving a maximum of ≈ 100 μJ per pulse around 308 nm with a bandwidth of 0.25 cm^{-1}. We used irises to produce a beam of 2×10^{-2} cm^2 cross-sectional area. At the interaction volume the energy of the pump pulses were typically less than 50 μJ and were constant over the wavelength region scanned. The overlap length was of the same order as the flame width. However, the centre of the interaction volume was arranged to be towards the far edge of the flame as viewed by the probe beam and so the signal generation volume was less than half of the flame width.

A 50 mm lens focused the DFWM signal through a small iris onto a photomultiplier tube. Simultaneous LIF data were recorded using a monochromator and photomultiplier tube positioned at 90° to the pump beams. The monochromator acted as an 18 nm bandpass filter centred at 309 nm and reduced the noise arising from the flame luminosity. Finally, a mirror directed the probe beam into a dye cell ≈ 5 m from the overlap region and a photodiode monitored the resulting fluorescence. This provided a measure of the absorption through the flame as well as monitoring the laser power over those wavelengths not in resonance with OH. The laser power/absorption, the DFWM and the LIF signals were recorded simultaneously on a PC which also controlled the laser scanning. For comparison CARS temperature measurements were made on the same flame on a separate occasion.

Measurements were made in a pre-mixed propane/air flame supported on a burner consisting of a rectangular plate in which 160, 1 mm diameter holes were drilled to give a flame of dimensions 1 cm wide by 10 cm long. This burner is routinely used to setup CARS experiments and is known to give reproducible flame conditions with a uniform temperature profile across the flame width. The beams traversed the width of the flame within 2 mm of the edge nearest the LIF detection chain. Hence absorption of the LIF signal could be neglected. The LIF and DFWM temperatures were determined using the R_1, R_{21} and R_2 branches of the $A^2\Sigma^+ - X^2\Pi_i$ band system of OH. These branches were chosen because they offer a large number of transitions within a 1 nm wavelength range and a wide variation of dipole moment.

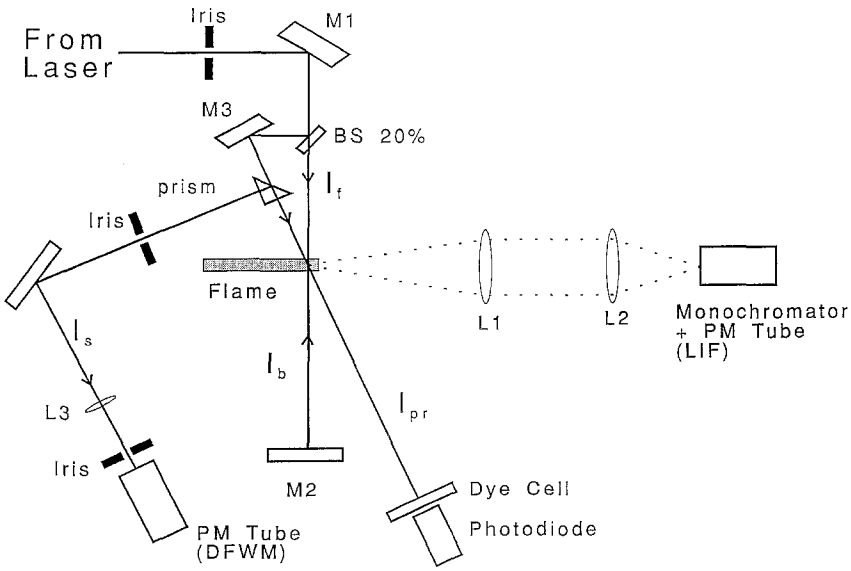

Fig. 1. Schematic of the simultaneous LIF and DFWM experiment. The DFWM optical arrangement is essentially the standard retro-reflected geometry but the use of misalignment has enabled the signal beam splitter to be replaced with a prism. See text for more details

2 Theory

Following the analysis of Farrow et al. [18] using a two level system, in the limit of a small amount of probe absorption and no absorption of the pump beams, the signal intensity, I_s, can be expressed for weak and strong pumps respectively, as:

$$I_s \propto (\Delta n)^2 \mu_{ij}^8 T_1^2 T_2^3 I^3, \quad I \ll I_{sat}, \tag{1}$$

$$I_s \propto (\Delta n)^2 \mu_{ij}^3 T_1^{-1/2} T_2^{1/2} I^{1/2}, \quad I \gg I_{sat}. \tag{2}$$

Here I is the non-monochromatic source-beam intensity, Δn the population difference in the absence of applied fields between level i and level j, μ_{ij} the transition dipole moment, T_1 the population decay time for the transition, T_2 the coherence decay time and I_{sat} the saturation intensity. For beam intensities that lie between the weak and strong limits, the dependence on dipole moment and laser power will be intermediate between them. This has important consequences for temperature determination as illustrated in the following analysis.

Using the relationships $I_s \propto n_i^2 \mu_{ij}^x$ [18] with $n_i \propto g_i \exp(-E_i/kT)$ and $\mu_{ij}^2 \propto B_{ij}$ [20], it is possible to express the DFWM signal intensity as a function of the rotational energy of the initial state:

$$\ln(\sqrt{I_s}/g_i B_{ij}^{x/4}) = -E_i/kT + \text{const.} \tag{3}$$

The temperature can be derived from a Boltzmann plot of the left-hand side of (3) against the rotational energy E_i. However, when $I \ll I_{sat}$, x is unknown, although it can be determined by rearrangement of (3) to give:

$$\ln(\sqrt{I_s}/g_i) + E_i/kT = \frac{x}{2} \ln \mu_{ij} + \text{const.} \tag{4}$$

Hence, a plot of the left-hand side of (4) against $\ln \mu_{ij}$ will yield the value of x. However, finding the value of x requires a prior knowledge of the temperature. We are thus left with the paradox that to determine the temperature the value of x must be known but to calculate x the temperature must be known.

This problem can be overcome in several ways depending on the data available. If the transitions scanned cover only a limited range of dipole moments, then (3) should be used to determine the temperature, optimising the linear regression fit to the data by varying the value of x. The alternative approach of estimating the temperature and using (4) will lead to large errors. If, on the other hand, the data cover a wide range of dipole moments, (3) or (4) can be plotted and the fits optimised by varying x or T, respectively. The corresponding derived values of T and x should then agree.

As an alternative, it is possible to pursue an iterative process using an initial estimate of x in (3) to determine an initial T, followed by a more accurate determination of x using the new temperature in (4). This is then repeated until the two equations converge to single values of x and T.

In the experiments described in this paper, significant beam absorption (10–15%) through the flame requires the above equations be modified. For a flame of length L the intensities of the two pump beams, the probe beam (crossing at an angle θ to the forward pump) and the signal generated at a point l will be reduced by absorption according to the Beer-Lambert law:

$$I_b = I_f^{(0)} \exp\left[\int_0^L -\varepsilon c(l)\,dl\right] \exp\left[\int_0^{L-l} -\varepsilon c(l)\,dl\right], \tag{5}$$

$$I_{pr} = I_{pr}^{(0)} \exp\left[\int_0^{l/\cos\theta} -\varepsilon c(l)\,dl\right], \tag{6}$$

etc.,

where $I_f^{(0)}$ and $I_{pr}^{(0)}$ are the forward pump and probe intensities before entering the flame and ε is the absorption coefficient. The $\cos\theta$ term in (6) arises from the projection of the probe beam on to the major axis defined by the pump beams. In this work, measurements were taken in the post flame region where the concentration of OH could be taken as constant over the length L. The above equations thus simplify to:

$$I_b = I_f^{(0)} \exp[-\alpha(2L-l)], \tag{7}$$

$$I_{pr} = I_{pr}^{(0)} \exp(-\alpha l/\cos\theta), \tag{8}$$

etc.,

where α is the product of the absorption coefficient and the constant concentration.

The signal generated at the interaction zone is proportional to $I_f I_b I_{pr} n_i^2 \mu^x$ and so the observed signal is given by:

$$I_s \propto (I_f^{(0)})^2 I_{pr}^{(0)} n_i^2 \mu_{ij}^x \exp[-2\alpha(L\cos\theta + l)/\cos\theta], \tag{9}$$

which is of similar form to the equation obtained by Ewart and O'Leary [21]. To obtain a temperature using a Boltzmann plot, the observed intensities must first be modified by the exponent of (9). As will be observed, failure to do so can give temperatures greater than those expected.

A similar correction must also be considered for LIF data. Here the signal is directly proportional to the laser intensity, which in this work can be taken as that of the two pump beams alone. A similar treatment to that for DFWM above leads to:

$$I_{LIF} \propto I_f^{(0)} n_i \mu_{ij}^2 \{\exp(-\alpha l) + \exp[-\alpha(2L-l)]\}, \tag{10}$$

where absorption of the fluorescence has not been included because of the close promixity of the measurement volume to the edge of the flame and the wide spread collisional redistribution of the excited state population [22]. Values of α for each transition were calculated using the absorption spectra collected simultaneously with the DFWM and LIF data.

3 Results and Analysis

Figure 2 shows an example of the simultaneously generated LIF and DFWM spectra of the R branches of OH in the propane/air flame. Each spectral point is an average of five laser shots. By recording the spectra at different laser powers a cubic dependence of DFWM signal on laser power, and a linear dependence for LIF was established. This confirmed that we were operating in the non-saturating regime.

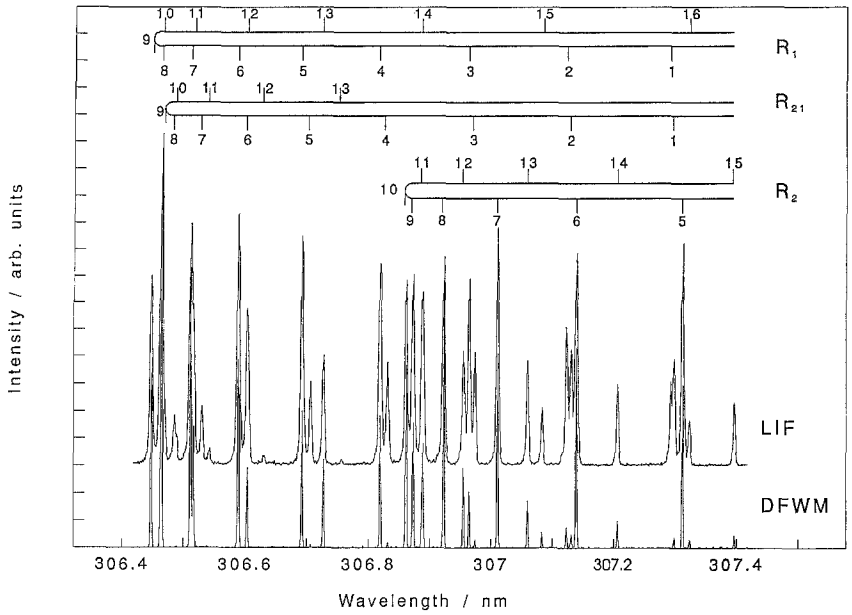

Fig. 2. OH DFWM and LIF spectra for the R_1, R_2 and R_{21} branches around 307 nm from a pre-mixed propane/air flame. The LIF spectrum has been offset for clarity. The step size was 0.0004 nm and each point is the average of 5 laser shots

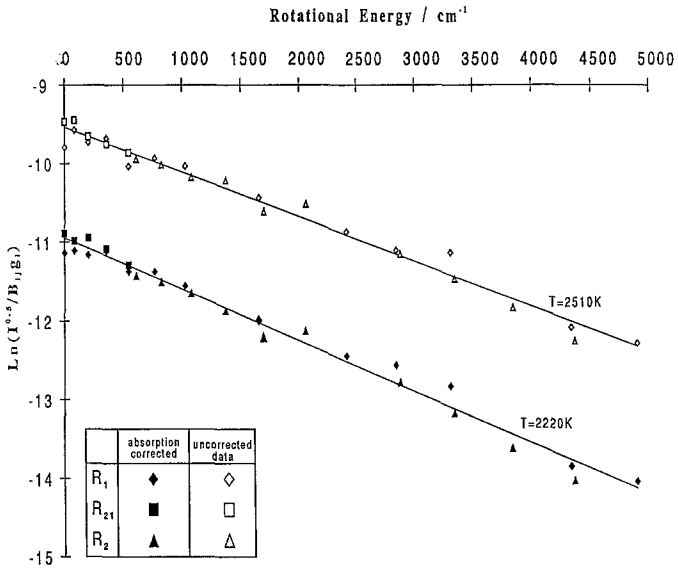

Fig. 3. Boltzmann plot for the DFWM spectrum of the R_1, R_2 and R_{21} branches of OH following the iteration between temperature and dipole moment power. The filled symbols are for data that have been corrected for absorption through the flame. The *solid lines* are linear regression fits to the corrected and uncorrected data. The two fits yield temperatures of 2220 K and 2510 K for the absorption-corrected and uncorrected data, respectively. The values of the dipole moment power used were 8.2 and 7.1, respectively (see Fig. 4)

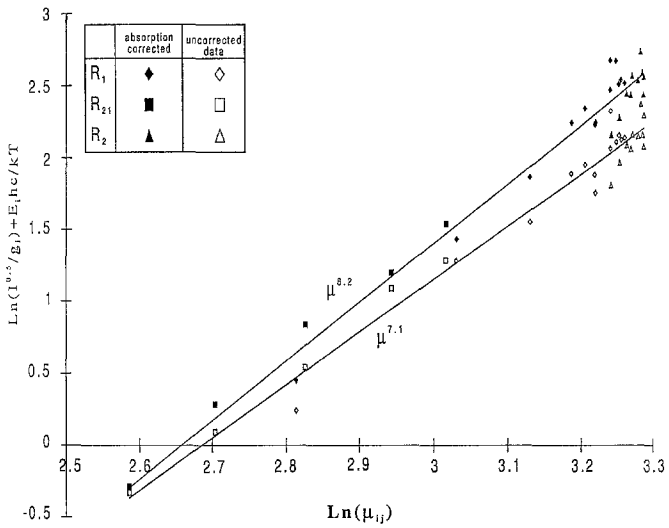

Fig. 4. Resulting dipole moment power plot for the DFWM spectrum of the R_1, R_2 and R_{21} branches of OH following the iteration between temperature and dipole moment power. The legend is the same as in Fig. 3. The two fits yield powers of 8.2 and 7.1 for the absorption-corrected and uncorrected data, respectively. The values of the temperatures used were 2220 K and 2510 K, respectively (see Fig. 3). Relative dipole moments are calculated using $\mu_{ij}^2 \propto B_{ij}$

The analysis of the DFWM data followed the iterative procedure described earlier. Figures 3 and 4 show a Boltzmann plot and the corresponding dipole moment plot for DFWM of OH. The figures show both absorption-corrected and uncorrected data; Einstein B coefficients have been taken from [23]. The temperature calculated from the corrected data is 2220 ± 60 K, which is in excellent agreement with the value of 2230 ± 60 K obtained using CARS. All errors quoted for the LIF and DFWM data are derived from regression analyses. Reproducibility of the data was confirmed by recording multiple spectra. These data gave agreement to within 50 K. The power of the dipole moment x derived from the corrected data is 8.2 ± 0.2 which agrees very well with the theoretically predicted value of 8 for weak beams. In comparison the uncorrected data given a temperature and a dipole moment power of 2510 ± 70 K and 7.1 ± 0.2, respectively. This illustrates the large influence absorption through the medium has over temperature accuracy. Note also that if only data from the R_2 branch were

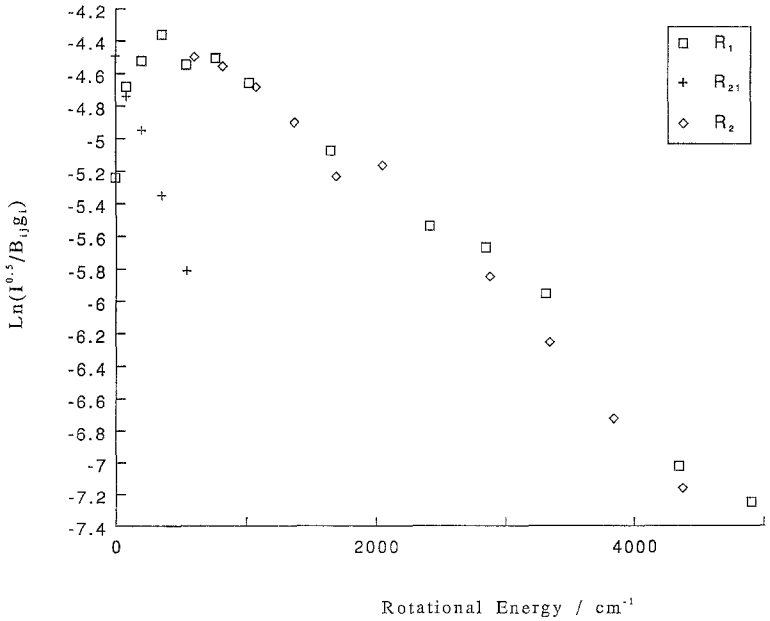

Fig. 5. Boltzmann plot for the DFWM spectrum of the R_1, R_2 and R_{21} branches of OH assuming a dipole moment power of 4 as opposed to 8.2. The difference between the satellite R_{21} branch and the main R_1 and R_2 branches is now clear, illustrating the importance of using the correct dipole moment power

available, the narrow spread in dipole moment would make it impossible to determine x, and thus the temperature, accurately.

The importance of using the correct value of x is vividly illustrated in Fig. 5 which shows the Boltzmann plot for the same data as used in Fig. 3 but assuming a dipole moment power of 4, as observed in the high power limit when $I \gg I_{sat}$ [13]. In this case the behaviour of the main R_1 and R_2 branches is completely different to that for the R_{21} branch and the deviation from a linear plot at low values of J renders any temperature derived from the plot meaningless.

The temperature of the flame was also determined from the LIF data. Figure 6 shows a Boltzmann plot for the LIF spectrum of OH shown in Fig. 2. The figure shows both raw data and data that have been corrected for absorption. The correction was made on the basis that the signal collected was generated at the rear edge of the flame after the beams had traversed the full width of the flame. Note that there is considerable variation in the slope, and hence temperature, between the R_{21} satellite lines and the R_1 and R_2 branches in the data that have not been corrected for absorption. This discrepancy is not observed after correction. The temperatures derived from the slopes of the two plots are 2040 ± 40 K and 2130 ± 60 K for the absorption corrected and uncorrected data respectively showing that failure to correct for beam absorption in LIF can, as with DFWM, lead to a significantly different temperature.

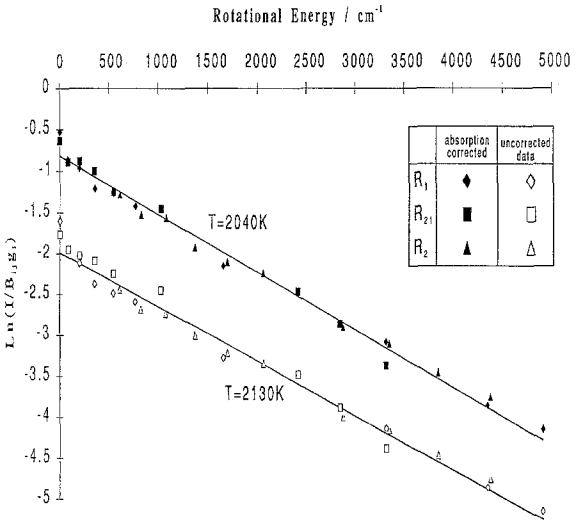

Fig. 6. Boltzmann plot of the R_1, R_2 and R_{21} branches of OH from the LIF spectrum shown in Fig. 2. The legend is the same as in Fig. 3. The two fits yield temperatures of 2040 ± 40 K and 2130 ± 60 K for the absorption-corrected and uncorrected data, respectively

We note with interest that the temperatures determined from LIF spectra in this region are consistently around 200 K lower than the equivalent DFWM and CARS temperatures. This appears to be due to the imperfect operation of the monochromator as a band pass filter which may arise from the polarisation sensitivity of the diffraction grating. Subsequent experiments used a UG11 Schott glass filter in place of the monochromator and resulted in a LIF spectrum which, despite the increased noise from the flame luminosity, gave a temperature of 2170 ± 70 K after absorption correction. This is in broad agreement with the CARS and DFWM temperatures.

Next we consider the importance of knowing accurately the position (l) of signal generation in the flame for accurate temperature determination using DFWM. Figure 7 shows a theoretical simulation of how the value of l (assuming signal generation from a single point) used for absorption correction, would change the fitted temperature from a given data set. A difference of 80 K would arise in the DFWM temperatures obtained at two positions only 1 cm apart. In contrast the LIF temperature would show a change of only 7 K.

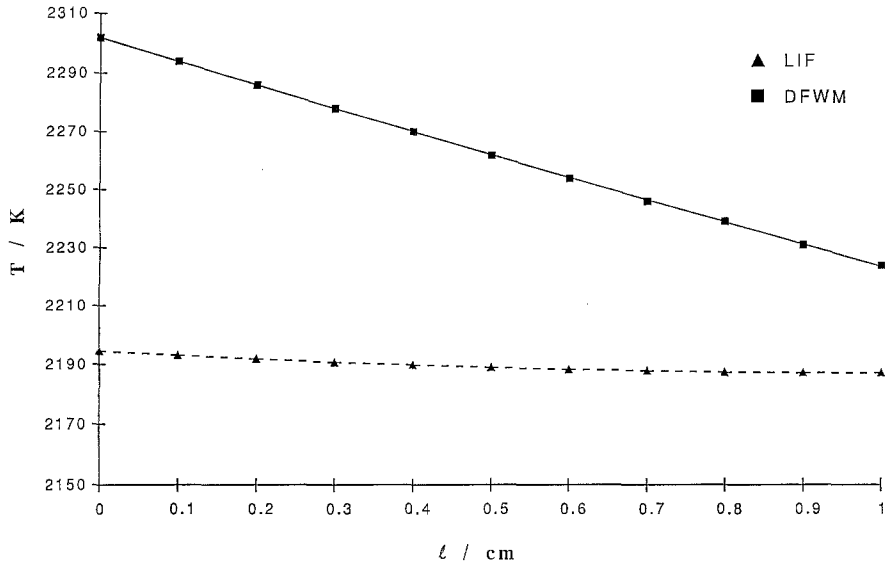

Fig. 7. Plot of the measured temperature against distance through the flame for both DFWM and LIF, illustrating the significant effect of absorption on the DFWM temperature. The *solid line* is a simulation of the effect for DFWM using (13) while the *dashed line* is present only as a visual aid for the LIF data

The form of the DFWM plot shown in Fig. 7 can be reproduced if we consider (3) for two particular transition, labelled 1 and 2, each modified to account for absorption. For transition 1 we have:

$$\ln\left(\frac{\sqrt{I_1}}{g_1 B_1^{x/4}}\right) + \frac{\alpha_1(\cos\theta + l)}{\cos\theta} = \frac{-E}{kT} + \text{const.} \tag{11}$$

with an analogous expression being written for transition 2. Combining the two gives:

$$\ln\left(\frac{\sqrt{I_1}}{g_1 B_1^{x/4}}\right) - \ln\left(\frac{\sqrt{I_2}}{g_2 B_2^{x/4}}\right) + \frac{(\alpha_1 - \alpha_2)(\cos\theta + l)}{\cos\theta}$$

$$= \frac{E_2 - E_1}{kT}. \tag{12}$$

This equation can be rearranged to give:

$$T = \frac{A}{B + Cl}, \tag{13}$$

where A, B and C are collections of terms that are independent of l or, like the measured signal intensity, have already been determined. Taking two transitions that lie on the Boltzmann line enable A, B and C to be determined. The solid line in Fig. 7 represents this equation with values of A, B and C equal to 5742, 2.494 and 0.088, respectively, calculated using the $R_1(6)$ and $R_1(16)$ transitions. Thus, in the case of DFWM, both experiment and theory show that the position of measurements within the flame has a much larger effect on the measured temperature than with LIF.

The above analysis is for the idealised situation of a single point signal source. In reality, however, signal is generated over a length determined by the overlap of the beams. In this case (5) and (6) (and the analogous ones for the other beams) would have to be integrated over the interaction length accounting also for the beam profiles. The key point is that the absorption correction necessary to obtain the correct DFWM temperature is only valid at one position within the flame and, as shown above, any error in the measurement position relative to the particular absorption correction used will lead to significant errors in the measured temperature. Thus in any application involving a flame whose dimensions are larger than the interaction length a knowledge of the measurements position would be essential to obtained the correct DFWM temperature.

Finally, for completeness, the temperature from the absorption spectrum was also calculated and found to be 2100 K. It should be noted however, that this is a line integral of the temperature through the flame and so detailed comparison with the more spatially resolved temperatures given by CARS, LIF and DFWM is inappropriate.

Clearly, working in a non-saturating regime ($I \ll 1$ MW/cm^2 per wavenumber [13]) presents many problems in the application of DFWM in practical environments where combustion devices may be several meters wide thus causing extensive beam absorption. In such circumstances the laser power at the interaction volume, the dipole moment power and the temperature will all be unknown. The laser power is the most crucial and the most difficult to establish, generally being estimated from line-of-sight absorption measurements through the flame.

One solution to these problems would be to implement DFWM in the non-saturating limit of weak beams where theory predicts a μ^8 dependence. However, work by Farrow et al. [18] has shown that dipole moment powers in excess of 10 can occur in NO. Although such behaviour in OH has not been reported to date, it cannot be entirely ruled out at this stage. Therefore this idealised approach may not be appropriate. It should also be noted that not all transitions will have the same dipole moment and so there will be a distribution of I_{sat} values throughout the spectrum. This means that in the intermediate power regime between $I \ll I_{sat}$ and $I \gg I_{sat}$, the dipole moment x may no longer be a constant across the spectrum.

Many of these problems, however, disappear when

working in a strongly saturating regime. Workers have found experimentally that the dipole moment power is four in such circumstances [13, 18] thus removing one unknown. Also, providing centre line intensities are used in subsequent analyses and in the limit of monochromatic radiation, there is no dependence on laser power [18] so absorption of the incoming beams can be ignored. However, if integrated peak areas are used, the resulting signal intensity is dependent on $I^{1/2}$ (2) and so correction for absorption of the input beams again becomes necessary. Signal absorption will still need to be considered in all cases. For molecules such as NO, which require higher laser intensities to achieve saturation, the iterative procedure outlined in this work may be necessary.

Perhaps the most significant area where the problems illustrated by this work will be most acute is in imaging applications of DFWM. The act of expanding the beams into sheets will inevitably lead to wide variations in power density across the sheet. Prior knowledge of the power density at each point in the interaction volume would then be required to be certain that saturation was being achieved at each point in the image. If not, the image may have to be corrected, with the dipole moment power determined at each point.

4 Conclusions

CARS, LIF and DFWM have been used on the same premixed propane/air flame to provide comparative measurements of temperature. All three techniques gave a temperature within 30 K of 2200 K and are in agreement with the accepted value for the propane/air flame temperature [24, 25]. The DFWM data show a dependence on the dipole moment of $\mu^{8.2}$ which is indicative of the use of low laser powers such that $I \ll I_{sat}$. We have shown that failure to establish the correct power of the dipole moment can result in, at best, inaccurate temperatures and, at worst, meaningless Boltzmann plots (although whether an inaccurate temperature is better than no temperature at all is a matter for debate beyond the scope of this paper). To determine the dipole moment power however, requires a knowledge of the temperature. A number of solutions to this apparent paradox have been presented.

We have also discussed the role of absorption in DFWM OH thermometry. Our data show that absorption in the $A \leftarrow X$ (0–0) band of OH cannot be neglected at the low laser powers used and that to do so can lead to a significant overestimate in the measured temperature. Furthermore, the accuracy of the absorption corrected DFWM temperature is found to be critically dependent on the accuracy with which the measurement position within the flame is known. An uncertainty of 1 cm, for instance, in the measurement position would lead to an error of 80 K in the flame used in this work, whereas the same uncertainty would lead to a change of only 7 K in the LIF temperature measurement.

This work confirms that it is preferable to operate with laser power densities well above those required for saturation when using DFWM for thermometry. In addition, working in such a power regime is also known to limit the effects of collisional quenching on DFWM [26]. These high power densities have significant implications for DFWM temperature mapping where local variations in the power density across the expanded laser sheets may lead to regions where the power density falls below the level required to saturate the OH transitions. This will in turn translate into wide variations in the dipole moment dependence and therefore wide variations in the temperature measured. The problem is compounded by the fact that the required saturation intensity, I_{sat}, is itself a function of pressure [14]. In combustion environments such as an internal combustion engine the pressure is an ever changing parameter. The laser intensity would then have to be in excess of the largest value of I_{sat}. Recent work has also shown that DFWM is sensitive to laser mode quality [27] which in conjunction with this work means that if the technique is to progress out of the laboratory into the industrial sector the advent of affordable and reliable high power single mode lasers is a pre-requisite.

Acknowledgements. The authors would like to thank the CEC for funding this work under the JOULE II programme (contract JOUE-CT91-0085). Thanks also to Sandy Yates and Richard Williams from the Clarendon Laboratory, Oxford for useful discussions on the relative merits of misaligned DFWM.

References

1. A.C. Eckbreth: *Laser Diagnostics for Combustion Temperature and Species* (Abacus, Cambridge, MA 1988)
2. D.A. Greenhalgh: In *Advances in Nonlinear Spectroscopy*, ed. by R.J.H Clark, R.E. Hester (Wiley, New York 1988) Chap. 5
3. M.J. Dyer, D.R. Crosley: Opt. Lett. **7**, 382 (1982)
4. W. Ketterle, M. Schäfer, A. Arnold, J. Wolfrum: Appl. Phys. B **54**, 109 (1992)
5. P. Andresen, G. Meijer, H. Schlüter, H. Voges, A. Koch, W. Hentschel, W. Oppermann, E. Rothe: Appl. Opt. **29**, 2392 (1990)
6. M.P. Lee, P.H. Paul, R.K. Hanson: Opt. Lett. **11**, 7 (1986)
7. M.G. Allen, R.D. Howe, R.K. Hanson: Opt. Lett. **11**, 126 (1986)
8. A. Arnold, B. Lange, T. Bouché, T. Heitzmann, G. Schiff, W. Ketterle, P. Monkhouse, J. Wolfrum: Ber. Bunsenges. Phys. Chem. **96**, 1388 (1992)
9. P. Ewart, S.V. O'Leary: Opt. Lett. **11**, (1986)
10. P. Ewart, P. Snowdon, I. Magnusson: Opt. Lett. **14**, 563 (1989)
11. E. Domingues, M.-J. Cottereau, D.A. Feikema: Third Int'l Symp. on Special Topics in Chemical Propulsion: Non-Intrusive Combustion Diagnostics, May 10–14, Scheveningen, The Netherlands (1993)
12. M. Winter, P.P. Radi: Opt. Lett. **17**, 320 (1992)
13. T. Dreier, D.J. Rakestraw: Appl. Phys. B **50**, 479 (1990)
14. R.L. Vander Wal, R.L. Farrow, D.J. Rakestraw: In *Proc. 24th Int'l Symp. on Combustion* (The Combustion Institute, Pittsburg, PA 1992)
15. B.A. Mann, S.V. O'Leary, A.G. Astill, D.A. Greenhalgh: Appl. Phys. B **54**, 271 (1992)
16. S. Williams, D.S. Green, S Sethuraman, R.N. Zare: J. Am. Chem. Soc. **114**, 9122 (1992)
17. G. Hall, A.G. Suits, B.J. Whitaker: Chem. Phys. Lett. **203**, 277 (1993)
18. R.L. Farrow, D.J. Rakestraw, T. Dreier: J. Opt. Soc. Am. B **9**, 1770 (1992)

19. T. Dreier, D.J. Rakestraw: Opt. Lett. **15**, 72 (1990)
20. R.C. Hilborn: Am. J. Phys. **50**, 982 (1982)
21. P. Ewart, S.V. O'Leary: J. Phys. B **17**, 4595 (9184)
22. K. Kohse-Höinghaus: Appl. Phys. B **50**, 455 (1990)
23. I.L. Chidsey, D.R. Crosley: J. Quant. Spectrosc. Radiat. Transfer **23**, 187 (1980)
24. B. Lewis, G. von Elbe: *Combustion, Flames and Explosions of Gases* (Academic, New York 1961)
25. J.A. Barnard, J.N. Bradley: *Flame and Combustion* (Chapman and Hall, London 1985)
26. P.M. Danehy, E.J. Friedman-Hill, R.P. Lucht, R.L. Farrow: Appl. Phys. B **57**, 243 (1993)
27. N.P. Tait, R.D. Bush, D.A. Greenhalgh: In *Multidimensional Imaging Diagnostics for Combustion II*, Second Periodic Report, ed. by J.O.W. Norris, CEC Contract JOUE-CT91-0085 (1993)